Distinct requirements for intra-ER sorting and budding of peroxisomal membrane proteins from the ER

Gaurav Agrawal, Scott N. Fassas, Zhi-Jie Xia, and Suresh Subramani

Section of Molecular Biology, Division of Biological Sciences, University of California, San Diego, La Jolla, CA 92093

During de novo peroxisome biogenesis, importomer complex proteins sort via two preperoxisomal vesicles (ppVs). However, the sorting mechanisms segregating peroxisomal membrane proteins to the preperoxisomal endoplasmic reticulum (pER) and into ppVs are unknown. We report novel roles for Pex3 and Pex19 in intra–endoplasmic reticulum (ER) sorting and budding of the RING-domain peroxins (Pex2, Pex10, and Pex12). Pex19 bridged the interaction at the ER between Pex3 and RING-domain proteins, resulting in a ternary complex that was critical for the intra-ER sorting and subsequent budding of the RING-domain peroxins. Although the docking subcomplex proteins (Pex13, Pex14, and Pex17) also required Pex19 for budding from the ER, they sorted to the pER independently of Pex3 and Pex19 and were spatially segregated from the RING-domain proteins. We also discovered a unique role for Pex3 in sorting Pex10 and Pex12, but with the docking subcomplex. Our study describes an intra-ER sorting process that regulates segregation, packaging, and budding of peroxisomal importomer subcomplexes, thereby preventing their premature assembly at the ER.

Introduction

Earlier studies proposed that peroxisomes form only by growth and division of preexisting peroxisomes (Lazarow and Fujiki, 1985; Lazarow, 1989). However, this traditional concept of peroxisome biogenesis has undergone a paradigm shift (Agrawal and Subramani, 2013). Numerous studies have presented morphologic (Hoepfner et al., 2005) and biochemical (Lam et al., 2010; Agrawal et al., 2011; van der Zand et al., 2012) evidence highlighting a central role of the ER in de novo biogenesis of peroxisomes. Importantly, fluorescence-tagged peroxisomal membrane proteins (PMPs) were localized at the ER in cells devoid of peroxisomes (Hoepfner et al., 2005; van der Zand et al., 2010) and were rerouted to the peroxisomes generated de novo (Yan et al., 2008; Agrawal et al., 2011). Later biochemical studies identified vesicular carriers that transport these PMPs out of the ER (Lam et al., 2010; Agrawal et al., 2011). These carriers either mature into functional peroxisomes or fuse with the preexisting peroxisomes (Titorenko and Rachubinski, 2000; van der Zand et al., 2012).

Two distinct preperoxisomal vesicle (ppV) carriers were characterized and found to contain either the RING-domain (comprising Pex2, Pex10, and Pex12) or docking subcomplexes (mainly Pex13, Pex14, and Pex17), which together constitute components of the peroxisomal importomer complex (van der Zand et al., 2012). These vesicles undergo heterotypic fusion in a manner dependent on the AAA-ATPases Pex1 and Pex6 (Faber et al., 1998; Titorenko and Rachubinski, 2000) to form a functional importomer complex, enabling the fused vesicle to import peroxisomal matrix proteins, thereby transforming it into a metabolically active organelle. An undefined sorting process has been proposed to exist at the ER to segregate these subcomplexes into distinct ppVs (Tabak et al., 2013; Kim and Hettema, 2015).

Pex19 and Pex3 are two peroxins that are central for PMP biogenesis and have multifaceted functions. Pex19, a predominantly cytosolic protein, binds PMP targeting signal (mPTS) sequences present on most PMPs and is considered to be a PMP chaperone that sequesters PMPs and prevents them from becoming unstable or aggregating in the cytosol after their synthesis (Shibata et al., 2004; Kashiwayama et al., 2005). In this role, Pex19 shuttles these PMPs to peroxisomes, where they are inserted into the peroxisome membrane. In mammalian cells, where growth and division is still the prevalent model for peroxisome biogenesis (Fujiki et al., 2014), Pex19 binds and stabilizes PMPs in the cytosol and delivers them to peroxisomes by docking with Pex3, an integral PMP, followed by membrane insertion of the PMPs (Fang et al., 2004). Structural analysis of Pex19 has revealed distinct binding sites for Pex3 in its N-terminal domain and an mPTS binding site in the C-terminal region (Fransen et al., 2005; Sato et al., 2010). Such spatial separation of the binding sites could enable the simultaneous interaction of Pex19 with Pex3 and other PMPs, supporting the claim that Pex19 incorporates PMPs into the peroxisomal membrane by docking on Pex3. In yeast, however, a novel

Correspondence to Suresh Subramani: ssubramani@ucsd.edu

Abbreviations used in this paper: 20P, 20,000 *g* pellet; 200S, 200,000 *g* supernatant; co-IP, coimmunoprecipitation; MIP, maximum-intensity projection; mPTS, PMP targeting signal; PIC, protease inhibitor cocktail; PMP, peroxisomal membrane protein; PNS, postnuclear supernatant; ppV, preperoxisomal vesicle; PYC, permeabilized yeast cell; WT, wild-type.

The Rockefeller University Press $30.00
J. Cell Biol. Vol. 212 No. 3 335–348
www.jcb.org/cgi/doi/10.1083/jcb.201506141

role of Pex19 in de novo peroxisome biogenesis is emerging (Agrawal and Subramani, 2013).

Independent studies using in vitro budding assays in yeast uncovered an essential role of Pex19 in the budding of ppVs from the ER (Lam et al., 2010; Agrawal et al., 2011), because ppV formation was dependent on Pex19. Nonetheless, budding could be restored when Pex19 was added. However, a direct role of Pex3 was not observed, as reactions lacking Pex3 still produced ppVs, although the budding of only one PMP, Pex11, was followed in these assays (Agrawal et al., 2011). With recent studies invoking a bipartite budding apparatus, the roles of Pex19 and Pex3 need to be reevaluated.

Recently, an intra-ER sorting signal in the N-terminal region of Pex3 was identified that targets it to the pER, and subsequent trafficking to the peroxisome requires the transmembrane segment of Pex3 (Fakieh et al., 2013). This implies that Pex3, by interacting with other PMPs at the ER, might escort them to the pER. However, such Pex3-mediated sorting for PMPs remains unproven.

In this study, we discovered novel roles of Pex3 and Pex19 in the intra-ER sorting and budding of RING-domain (Pex2, Pex10, and Pex12) and docking complex (Pex13, Pex14, and Pex17) PMPs. Specifically, Pex3 and Pex19 work in concert for the sorting to the pER—and budding—of the RING-domain proteins from the ER. In contrast, the docking complex proteins sort to the pER independently of Pex3 and Pex19 but require Pex19 for budding from the pER. This asymmetric requirement for intra-ER sorting and budding constitutes the basis for segregation of these PMPs at the pER into distinct ppVs. Importantly, this is the first direct role found for Pex3 in de novo peroxisome biogenesis. Our results also successfully integrate the classic role of Pex3 as the membrane-associated docking component for Pex19 in both biogenesis pathways.

Results

Pex19 and Pex3 play distinct roles in the budding of RING-domain and docking complex PMPs from the ER

Our previous study in *Pichia pastoris* (Agrawal et al., 2011) elucidated the role of Pex19 in the budding of ppVs containing the PMPs Pex11 and Pex3 from the ER. However, our discovery that Pex3 was not required for the budding of Pex11 from the ER was surprising, because Pex3 is viewed as the docking factor for Pex19 at the peroxisome membrane (Fang et al., 2004). In addition, vesicular fractions isolated from *pex3Δ* cells lacked the full repertoire of PMPs and matrix proteins representative of ppVs derived from the wild-type (WT) fractions. This further suggested a role of Pex3 in the intra-ER segregation of PMPs before ppV budding. Despite our finding, a mechanistic role of Pex3 in de novo peroxisome biogenesis was unclear.

Subsequently, PMPs were found to traffic in two distinct ppV carriers from the ER, one with the docking complex proteins, Pex13, Pex14, and Pex17 (ppV-D), and the other with the RING-domain proteins Pex2, Pex10, and Pex12 as well as Pex11 (ppV-R; van der Zand et al., 2012). A subsequent heterotypic fusion event between ppV-D and ppV-R, requiring the AAA-ATPases Pex1 and Pex6, reconstitutes the importomer complex to enable matrix protein import. In light of these results, we analyzed the budding requirements for these proteins. We tagged Pex2 and Pex17 with three tandem hemagglutinin tags (3HA) at their C termini. Similarly tagged Pex3 and Pex11 were included in the assays. The strains expressing these proteins had no deleterious effects caused by tagging or constitutive expression in that all the tagged proteins complemented their respective deletion strains (Fig. 1 A). The combinations of genetic backgrounds with respective HA-tagged PMPs are shown in Fig. 1 B.

Budding assays were performed as described previously (Agrawal et al., 2011). In brief, cells expressing the HA-tagged PMPs were induced for peroxisome biogenesis by growing on methanol for 3 h. Permeabilized yeast cells (PYCs) were prepared (see Materials and methods), and the budding reaction was initiated by adding the S1 fraction (crude cytosol) to the PYCs, with concomitant addition of an ATP-regenerating system and incubation at 20°C for 90 min. The S1 fraction supplies soluble factors necessary for budding in the presence of the ATP-regenerating system. In controls, PYCs were pretreated with apyrase to deplete ATP, before the addition of the S1 fraction. PYCs were separated from the released vesicular fraction by a brief centrifugation step; the supernatant was analyzed by SDS-PAGE and immunoblotting with a rat monoclonal antibody against the HA tag.

As expected from our previous results (Agrawal et al., 2011), we detected Pex3-3HA and Pex11-3HA in the ppV fraction obtained from WT cells (Fig. 1 C). In addition, we also detected Pex2-3HA and Pex17-3HA. However, in control reactions with apyrase, or when TBPS buffer was substituted for cytosol, the budding of PMPs was dramatically decreased or absent. In PYCs prepared from the *pex19Δ* cells, none of the PMPs showed significant budding. These results highlight an essential role for Pex19 in the trafficking of both docking complex and RING-domain PMPs to ppVs. Similar to our previous findings, Pex11-3HA was detected in the ppV fraction derived from the reaction with the *pex3Δ* PYCs. Most interestingly, however, Pex17-3HA, but not Pex2-3HA, was detected in this fraction. The apparent intensity for Pex17-3HA signal was lower in the budded ppV fraction, perhaps suggesting a somewhat reduced budding efficiency in the absence of Pex3. Nonetheless, these results clearly demonstrate an absolute requirement of Pex3 for the budding of Pex2, but not Pex17 or Pex11, from the ER.

We discovered that Pex11, like Pex17, did not require Pex3 for budding, implying that Pex11 could be associated with the ppV-D. This is in contrast to previously published data (van der Zand et al., 2012), in which Pex11 was copackaged in the ppV-R. Nonetheless, this is a first instance demonstrating a direct role of Pex3 in de novo peroxisome biogenesis.

Both Pex19 and Pex3 are required for sorting of Pex2 to the pER

To further assess the role of Pex3, the cellular localization of RING-domain and docking complex proteins were studied in various genetic backgrounds. Pex2, Pex17, Pex3, and Sec61 (ER marker) were fused to fluorescent tags and localized at specified time intervals after peroxisome induction (see Materials and methods). As expected, in WT cells switched to methanol medium, Pex2 and Pex17 were localized to the typical punctate clusters (Fig. 2, A and B; and Fig. 3, A and B) representing mature peroxisomes, well segregated from the Sec61-mCherry decorating the cortical and perinuclear ER. We also analyzed Pex17 expressed from the endogenous promoter (P_{PEX17}-Pex17-GFP) to ensure that ER-associated localization is not caused by

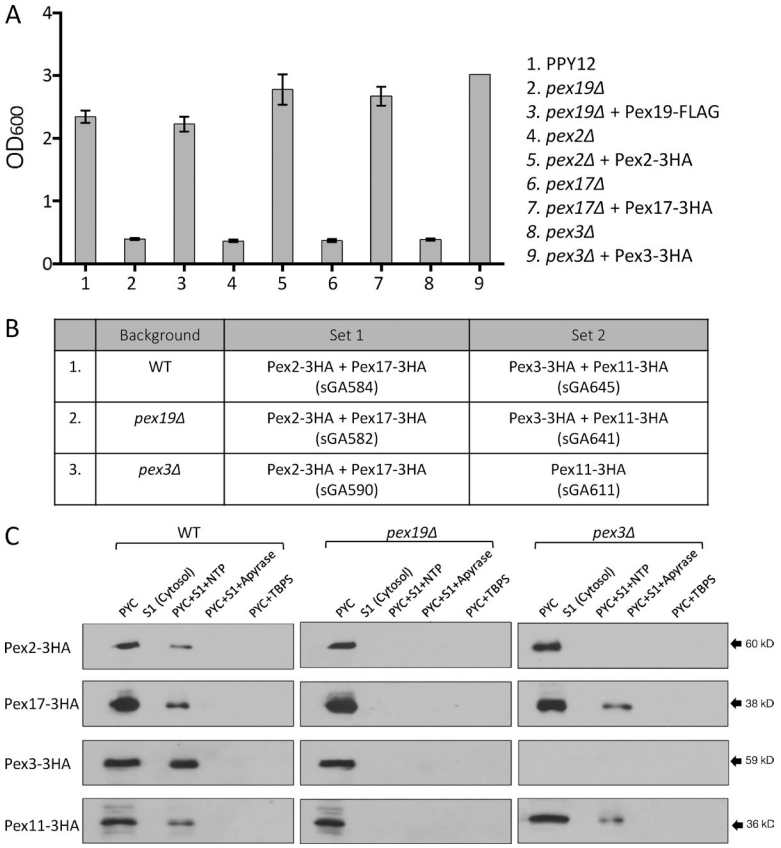

	Background	Set 1	Set 2
1.	WT	Pex2-3HA + Pex17-3HA (sGA584)	Pex3-3HA + Pex11-3HA (sGA645)
2.	*pex19Δ*	Pex2-3HA + Pex17-3HA (sGA582)	Pex3-3HA + Pex11-3HA (sGA641)
3.	*pex3Δ*	Pex2-3HA + Pex17-3HA (sGA590)	Pex11-3HA (sGA611)

Figure 1. **Pex3 is required for budding of the RING-domain protein Pex2 from the ER.** (A) Cells transformed with plasmids expressing specified HA-tagged proteins were assayed for growth on methanol medium. Cells were grown overnight in YPD, and ∼0.1 OD_{600}/ml was further inoculated into methanol medium. Cell growth was measured after 48 h. All the HA-tagged proteins complemented their respective deletion mutants. The assay was repeated twice with similar results. (B) Genetic backgrounds of the strains used in the budding assay in C. (C) ER-budding assays were performed as described in Materials and methods. Peroxisomal proteins in the budded ppVs were detected by immunoblotting. S1, supernatant cytosolic fraction; NTP, nucleoside triphosphates; TBPS, buffer control. 30 µl of 80-µl reaction was analyzed. Input is ∼10% of PYCs used in each reaction. The experiment was repeated three times with similar results.

overexpression of the PMP. As seen in Fig. 3 A, when cells were shifted to methanol medium (0 h), Pex17-GFP was localized at the cell periphery and occasionally formed a punctate structure over the perinuclear ER. This likely represents a subdomain of the ER (pER) where PMPs are localized before their exit (Hoepfner et al., 2005). Within 3 h, Pex17-GFP was entirely localized on the peroxisome cluster with no significant ER localization (Fig. 3 A), suggesting that Pex17-GFP traffics to the pER after being located all over the ER. Because the expression of Pex2-GFP was very low at early time points, we analyzed the trafficking of Pex2-GFP expressed from an inducible AOX promoter. P_{AOX}-Pex2-GFP followed a localization pattern similar to that of Pex17-GFP in WT cells (Fig. 3 B).

In contrast, PMPs in the *pex19Δ* and *pex3Δ* cells localized at or near the cortical ER (labeled with Sec61-mCherry; Fig. 2, A–C). However, the manner of mislocalization of the RING-domain and docking complex PMPs was distinct. On the one hand, Pex17 was at a distinct dot near the cortical and the perinuclear ER in both *pex19Δ* and *pex3Δ* cells, as well as in the *pex3Δ pex19Δ* double-mutant cells (Figs. 2 B and 3 A). In a maximum-intensity projection (MIP) image created from the superimposition of *Z*-stacks (∼30 frames), only one or few dots were seen in each cell (Figs. S1 A and S2 A). Because budding, and thus exit of Pex17, is blocked from the ER in *pex19Δ* cells, the punctate structure most likely represents the pER, where the PMPs accumulate before their exit from the ER (Hoepfner et al., 2005). In cells grown for longer periods (24 h) in methanol, the localization of Pex17 at the pER became nearly exclusive (Fig. S1A). In addition, small vesicular structures were not seen in *pex19Δ* cells, and the Pex17 punctum remained unchanged, because Pex19 is required for the budding of Pex17 (Figs. 1 C and S1 A). Most interestingly, in addition to the one bright pER punctum in each cell, apparent vesicular structures of lighter intensity were detected in *pex3Δ* cells, when Pex17-GFP was visualized, and when a MIP image was created from superimposition of *Z*-stacks (∼30 frames; Fig. S1 B). No such vesicular structures were observed when Pex2-GFP was visualized in either WT or *pex19Δ* cells (Fig. S2A). This further validated our budding assay results.

Interestingly, Pex3-RFP also displayed localization similar to that of Pex17-GFP in *pex19Δ* cells, further confirming that the punctate structure associated with the cortical ER is in fact the pER (Figs. 2 C and S2, A and C). Unlike Pex17-GFP, however, a fraction of Pex3-RFP was also dispersed around the cell periphery colocalizing with Pex2 (Fig. 2 C). These results suggest that the sorting of Pex17-GFP to the pER is independent of both Pex19 and Pex3, whereas the sorting of Pex3-RFP itself to the pER also does not require Pex19, consistent with the fact that Pex3 contains an intra-ER sorting signal (Fakieh et al., 2013). Nonetheless, the budding of both Pex17 and Pex3 requires Pex19 (Fig. 1 C).

Interestingly, Pex2 localization was different from that of Pex17 in *pex19Δ* and *pex3Δ* cells (Figs. 2 A and S2 A). Pex2 was uniformly distributed at the cortical ER (labeled with Sec61-mCherry) and without forming the punctate structures seen for Pex17 and Pex3. This localization did not change, and no punctate structure was formed even after 24 h in methanol medium. As stated earlier, in the *pex19Δ* cells, the majority of Pex3 was at the punctate pER, although some was also colocalized with Pex2 at the cortical ER (Fig. 2 C). The Pex2 localization with the *pex3Δ pex19Δ* double-mutant cells was similar to that observed in the single-mutant cells (Fig. 2 A). Thus, unlike Pex17 and Pex3, Pex2 requires both Pex3 and Pex19 for its

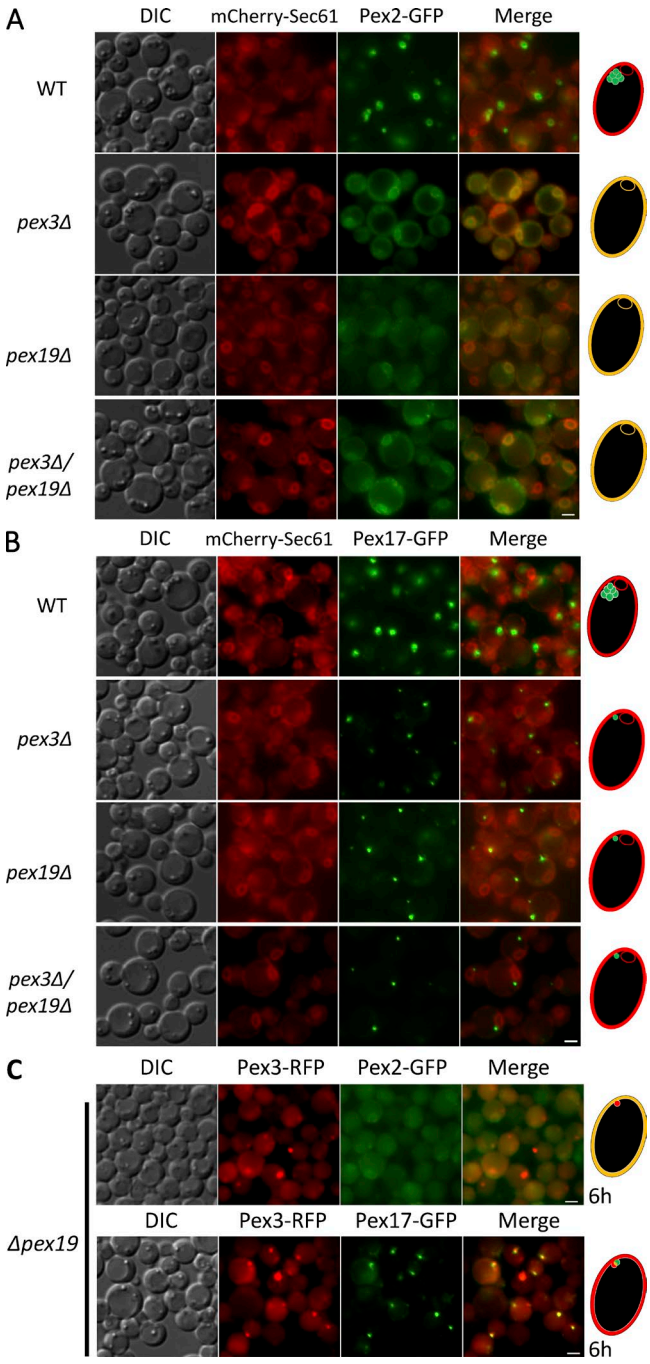

Figure 2. **Pex2-GFP and Pex17-GFP localization in WT and mutant cells.** Fluorescence microscopy analysis of methanol-grown cells (3 h) expressing Pex2-GFP or Pex17-GFP. Cells were grown in YPD and switched during exponential phase to methanol medium. DIC, differential interference contrast. Bar, 2 µm. (A) Colocalization of Pex2-GFP expressed from the inducible alcohol oxidase (AOX) promoter with the ER marker Sec61-mCherry in WT and mutant cells. (B) Colocalization of Pex17-GFP expressed from the inducible AOX promoter with the ER marker Sec61-mCherry in WT and mutant cells. (C) Localization of Pex2-GFP and Pex17-GFP with Pex3-RFP after 6 h in methanol medium. Each localization experiment was repeated more than five times with similar results.

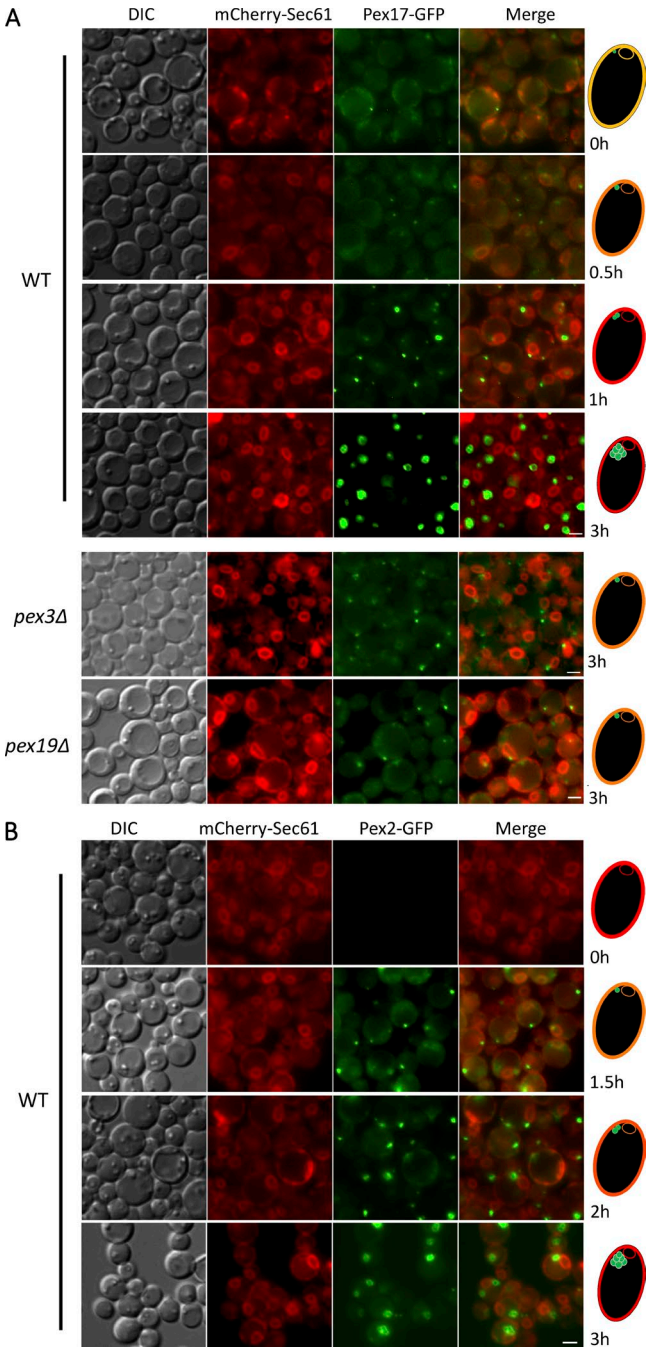

Figure 3. **Pex2-GFP and Pex17-GFP are trafficked through the ER.** (A) Colocalization of Pex17-GFP expressed from its endogenous promoter with the ER marker Sec61-mCherry in WT and mutant cells. (B) Colocalization of Pex2-GFP expressed from the AOX promoter with the ER marker Sec61-mCherry in WT cells at specified time points.

sorting to the pER. Extending the budding assay observations (Fig. 1), these results further indicate distinct requirements for the intra-ER sorting of RING-domain (Pex2) and docking complex (Pex17) PMPs.

Pex2-GFP and Pex17-GFP are exclusively membrane associated

In fluorescence microscopy imaging, in addition to peripheral-ER localization, a diffuse cytosolic signal was observed, especially for Pex2-GFP in mutant cells (Fig. 2 A). To rule out the possibility of cytosolic localization and direct import of Pex2-GFP and Pex17-GFP to the pER structures from the cytosol, we analyzed the membrane association of both Pex2-GFP and Pex17-GFP using subcellular fractionation. First, we analyzed TCA precipitates of intact cells, which showed

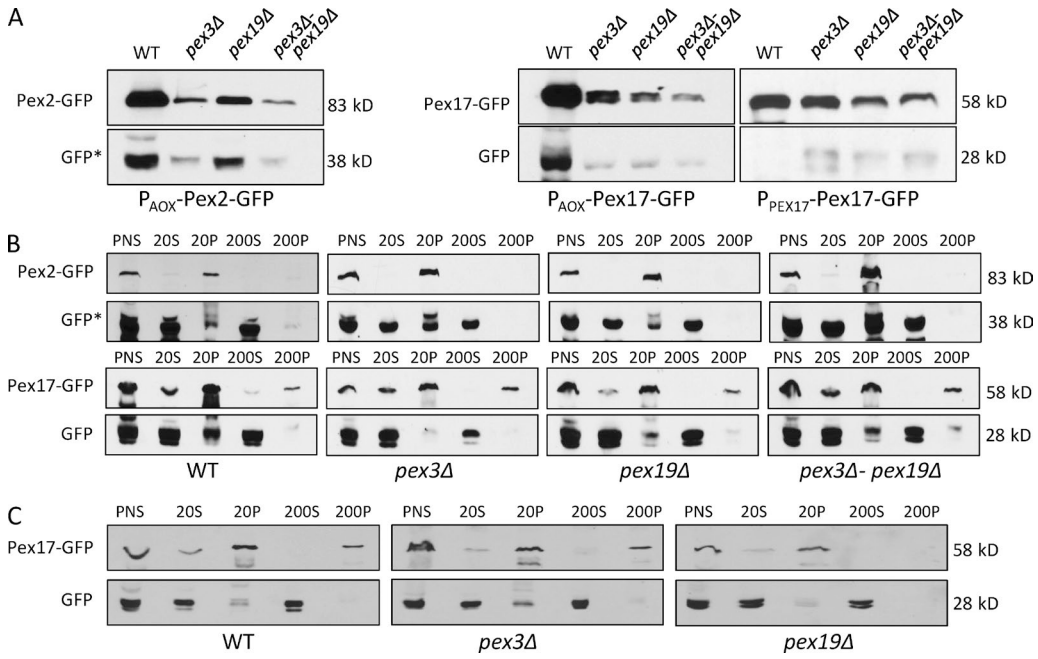

Figure 4. **Subcellular fractionation of Pex2-GFP and Pex17-GFP.** (A) TCA precipitates of intact cells expressing Pex2-GFP or Pex17-GFP from the specified promoter were obtained as described in Materials and methods. Western blotting was performed with anti-GFP monoclonal antibody. GFP* is the cleaved fragment of Pex2-GFP and is ~10 kD larger than the GFP fragment cleaved from Pex17-GFP. Notably, Pex17-GFP expressed from the endogenous promoter showed no significant cleavage. (B) Cells expressing Pex2-GFP or Pex17-GFP from the inducible AOX promoter were grown in methanol medium (8 h) and fractionated to obtain PNS, 20S, 20P, 200S, and 200P fractions as described in Materials and methods. The pellet fractions were resuspended in the initial volume, and equal volumes of each fraction was analyzed by SDS-PAGE and immunoblotting. (C) Cells expressing Pex17-GFP from endogenous promoter were fractioned and analyzed as described in B. All the subcellular fractionation experiments were repeated three times with similar results.

that a small fraction of both Pex2-GFP and Pex17-GFP was cleaved toward the C-terminal end, yielding smaller fragments containing GFP (Fig. 4 A). Interestingly, the cells expressing Pex17-GFP from its endogenous promoter showed significantly less cleavage. This could suggest that overexpression of PMPs promotes this intramolecular cleavage. However, the subcellular fractionation assays clearly demonstrated that both Pex2-GFP and Pex17-GFP were strictly membrane associated in all backgrounds because they were present exclusively in the pellet fractions (20,000 *g* pellet [20P] and 200P), presumably associated with ER, vesicles, or peroxisome membrane, and were completely absent from the cytosolic 200,000 *g* supernatant (200S) fraction (Fig. 4 B). PMPs present in the 20S fractions could be associated with vesicles or fragmented ER membranes as a result of the cell homogenization procedure. Interestingly, the GFP fragment was predominantly present in the 200S fraction (cytosol) and is the likely reason for diffuse cytosolic localization in fluorescence microscopy. In addition, the intramolecular cleavage was amplified during the cell fractionation procedure, probably because of a release of vacuolar proteases (Fig. 4 B).

Subcellular fractionation of strains expressing P_{PEX17}-Pex17-GFP showed very similar results (Fig. 4 C). Together, these results show an exclusive association of these PMPs with membrane fractions and rule out their direct import from the cytosol to the pER.

Pex2 and Pex17 sort to pER and eventually form small vesicular structures in pex1Δ and pex6Δ cells

The role of Pex3 and Pex19 for intra-ER sorting was further supported when Pex2 was localized in *pex1Δ* and *pex6Δ* cells. Pex1 and Pex6 are AAA-ATPases and are critical for fusion of the ppV-D and ppV-R (Titorenko and Rachubinski, 1998; van der Zand et al., 2012). Although the deletion of *PEX1* or *PEX6* does not block the budding of ppVs from the ER (Agrawal et al., 2011), functional peroxisomes are not formed in these mutants (van der Zand et al., 2012). In *pex1Δ* cells, both Pex2 and Pex17 localized to distinct punctate structures associated with the cortical ER (labeled with Sec61-mCherry) after 6 h in methanol medium, representing a pER domain (Fig. 5 B). Again, the MIP of *Z*-stacks showed only one or few prominent dots per cell for both Pex2 and Pex17 in *pex1Δ* cells, representing the pER, but now some vesicular structures were highly visible after 24 h (Figs. 5 A; S2, A and B; and S3 A). Thus Pex2 requires the presence of both Pex3 and Pex19 for sorting to the pER (Fig. 2 A). After 30 h in methanol medium, numerous small vesicular structures containing Pex2 were detected, perhaps formed from the pER site, as evident from the diminishing fluorescence of the punctum at the pER (Figs. 5 A and S3, A and B). Similar vesicular structures were observed with other PMPs, Pex3 and Pex11 (Fig. S3, A and B). This is markedly different from the observation in *pex19Δ* cells that the Pex17 punctum at the pER was not diminished, nor were any vesicular structures detected (Fig. 2, A–C), further confirming the identity of the punctate structure as the pER (because if the punctate structure in *pex1Δ* and *pex6Δ* cells were a peroxisome remnant, it should not have disappeared over time).

Interestingly, in *pex1Δ* and *pex6Δ* cells, the pER puncta containing Pex2 and Pex17 were very closely associated, although not colocalizing completely (Figs. 5 A and S2 B). This suggests distinct pER domains for Pex2 and Pex17. In addition, Pex3 puncta were more closely associated with Pex2 (Fig. S3 B), possibly suggesting overlapping localization at the pER.

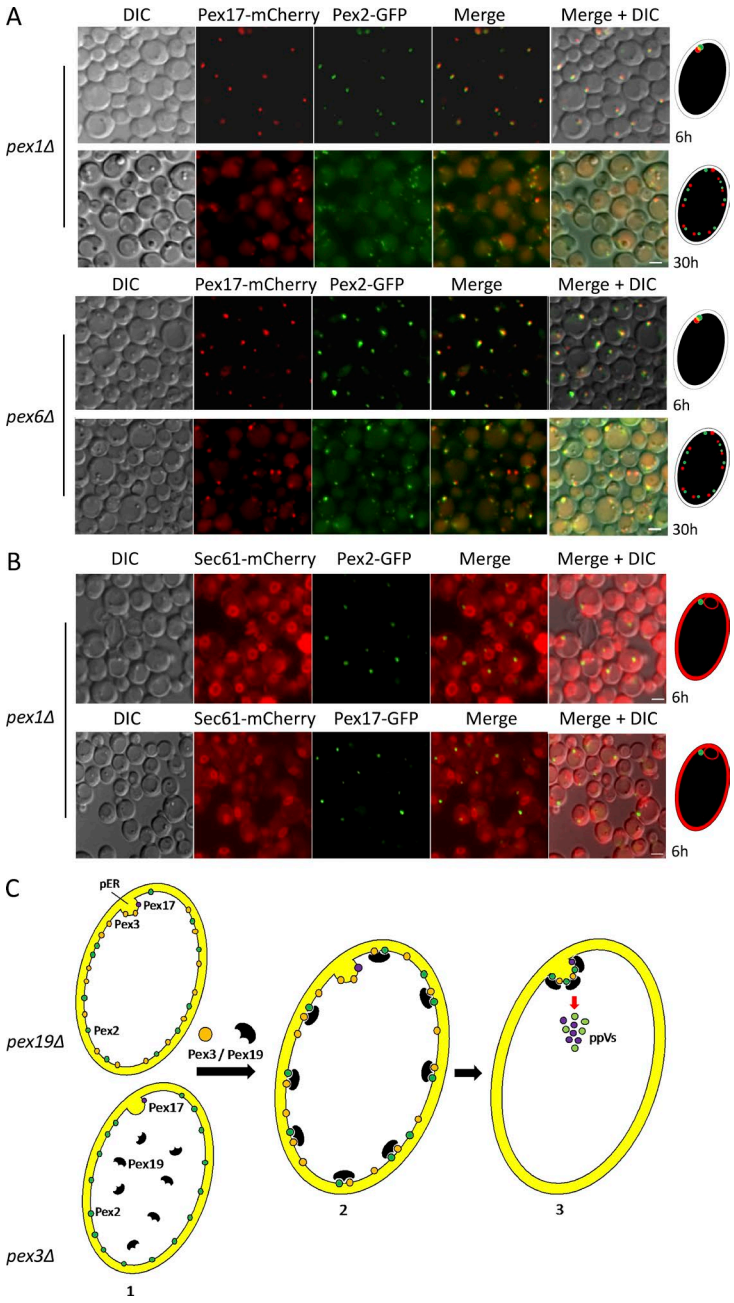

Figure 5. **Localization of Pex2 and Pex17 in *pex1Δ* and *pex6Δ* cells.** (A) Pex17-mCherry and Pex2-GFP localization in *pex1Δ* and *pex6Δ* cells. Bar, 2 µm. (B) Pex2-GFP and Pex17-GFP localization relative to Sec61-mCherry in *pex1Δ* cells. (C) Model summarizing the localization and sorting requirements for PMPs. Step 1 shows the RING-domain protein Pex2 dispersed at the cell periphery, whereas the docking complex proteins are sorted to the ER in cells lacking Pex3 or Pex19 (Fig. 2, A–C). Similar localization patterns were observed in *pex3Δ* cells, as well as in *pex3Δ pex19Δ* double mutants. However, when both Pex3 and Pex19 were reintroduced as seen in *pex1Δ* or *pex6Δ* cells, both Pex2 and Pex17 localized to the pER and subsequently budded out of the ER, forming ppVs as in A and B. Each localization experiment was repeated more than three times with similar results.

Association of Pex2 with Pex3 in *pex1Δ* and *pex6Δ*, but not in *pex19Δ*, cells suggested a requirement of Pex19 for their colocalization (further confirmed in Fig. 7 A). The roles of Pex3 and Pex19 in the intra-ER sorting Pex2 and Pex17 to the pER are summarized in Fig. 5 C.

Pex3 restores the interaction between Pex19 and the RING-domain proteins at the ER

The localization and budding assay experiments depicted an essential role of Pex3 in both intra-ER sorting and budding of Pex2, a RING-domain protein from the pER, whereas the docking protein, Pex17, was sorted to the pER and present in the ppVs isolated from *pex3Δ* cells.

Earlier studies highlighted the role of Pex3 as a docking protein for Pex19 on the peroxisomal membrane required for the peroxisomal insertion of PMPs ferried from the cytosol (Fang et al., 2004). However, during de novo peroxisome biogenesis, Pex19 functions differently and is required for the budding of ppVs from the ER (Lam et al., 2010; Agrawal et al., 2011), consistent with our suggestion that, in *P. pastoris*, Pex19 binds mPTSs on PMPs primarily in the membrane fraction and not in the cytosol, and that it might function to reorganize PMPs into membrane complexes (Snyder et al., 2000). Therefore, we assessed whether the role of Pex3 in the de novo pathway might be as a docking factor for Pex19 specifically at the pER membrane, which had not been tested. In addition, if Pex3 was exclusively required for Pex19 to dock with the RING proteins, the requirement of Pex3 for the sorting and budding of these PMPs might be explained.

We addressed this differential necessity of Pex3 by analyzing the requirement of Pex3 for the interaction between Pex19 with RING-domain and docking complex PMPs. Importantly, because *P. pastoris* Pex19 binds mPTSs on PMPs primarily in

the membrane fraction (Snyder et al., 2000), we analyzed the interaction using the membrane fraction.

Pex19 with a FLAG tag was expressed from the inducible alcohol oxidase promoter in *pex19Δ* (WT), *pex3Δ*, and *pex1Δ* cells. As expected, the stability of PMPs differed according to the specific backgrounds but was usually affected in *pex3Δ* cells (Fig. 6 A). Significantly, Pex2-GFP from the RING-domain protein complex and Pex13 and Pex14 from the docking protein complex were the most stable and comparable in all backgrounds. The coimmunoprecipitation (co-IP) results clearly suggested that Pex3 was required for a strong interaction between Pex19 and Pex2-GFP, but not for the interaction between Pex19 and Pex14. Similarly, interaction between another RING-domain protein, Pex12, and Pex19 was also strong when Pex3 was present (WT and *pex1Δ* cells), although the levels of Pex12 in *pex3Δ* cells were lower in comparison to WT. Most importantly, the interaction between all the RING-domain proteins and Pex19 was very strong in *pex1Δ* cells compared with *pex3Δ* cells. These backgrounds are more relevant because in both cases the interaction was tested between the ER-associated PMPs and Pex19, as the vesicular fraction was excluded from the 20P, which was tested. Thus, Pex3 strengthens the interaction between Pex19 and the RING-domain proteins at the ER membrane. However, the docking complex proteins, Pex13, Pex14, and Pex17, exhibited a strong interaction with Pex19, even in *pex3Δ* cells (Fig. 6 A).

These results, in conjunction with the budding assay and PMP localization experiments, provide a mechanistic understanding of the role of Pex3 in the de novo pathway. Presumably, Pex3 first recruits Pex19 at the ER membrane, enabling its stable interaction with the RING-domain proteins (Pex2/10/12; see also next section). Then, because Pex3 has an intra-ER sorting signal of its own (Fakieh et al., 2013), it can sort, with the help of Pex19, the RING-domain proteins to the pER (Fig. 6 B). The docking complex proteins (Pex13/14/17) do not require Pex3 for a stable interaction with Pex19 and thus sort to the pER without requiring Pex3 and bud into ppVs subsequently, in a reaction that requires only Pex19.

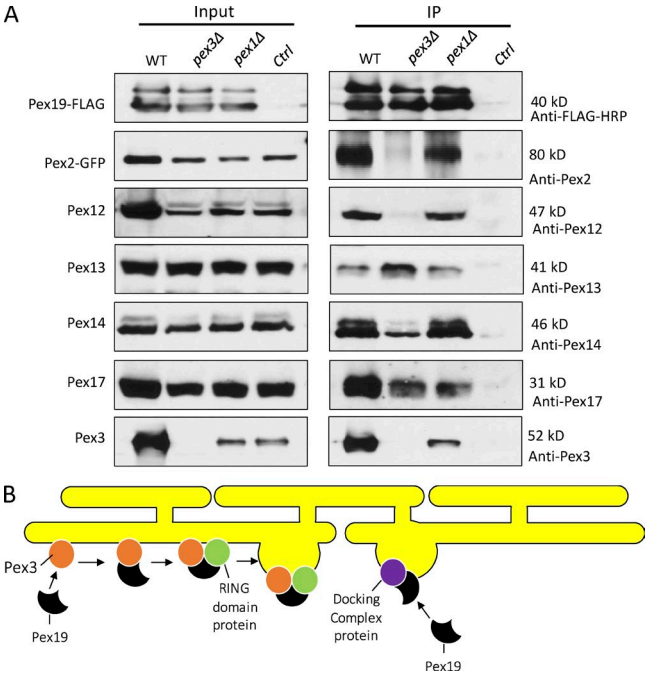

Figure 6. **Pex3 is required for the interaction between Pex19 and RING-domain proteins.** (A) Co-IP was performed by immunoprecipitating Pex19-FLAG using M2-agarose beads as described in Materials and methods. Immunoblotting was performed with the specified antibodies. The cells were harvested after 6 h in methanol medium. Co-IP was repeated three times with similar results. Ctrl, control; HRP, horseradish peroxidase. (B) Model summarizing the co-IP data. Pex19 presumably docks with Pex3 at the ER, enabling it to interact stably with the RING-domain proteins. This ternary complex initiates intra-ER sorting of the RING-domain proteins to the pER. This is evident from the localization of fluorescence-tagged Pex2 in *pex1Δ* cells, where in the presence of both Pex3 and Pex19, Pex2 sorts to a punctate pER structure (Fig. 5, A and B). Failure to sort to the pER in the absence of Pex3 could be the reason that the RING-domain proteins do not bud in *pex3Δ* cells. However, the docking complex proteins do sort and bud because they interact with Pex19 in the absence of Pex3.

Pex19 is required for the interaction between Pex3 and both RING-domain and docking complex PMPs

The RING-domain proteins mislocalized to the cortical ER in *pex19Δ* cells, whereas Pex3 was predominantly localized to a punctate structure. Thus, although Pex3 by itself can sort to the pER, Pex19 is necessary for the sorting of the RING-domain proteins, as exemplified by Pex2. We addressed this conundrum by testing the interaction of the RING-domain proteins with Pex3 in *pex19Δ* cells.

Co-IPs were performed by immunoprecipitating Pex3-3HA in WT, *pex19Δ*, and *pex1Δ* cells. *pex3Δ* and *pex1Δ* cells without Pex3-3HA were used as controls. In WT cells, Pex3-3HA showed a strong interaction with the RING-domain proteins Pex2, Pex10, and Pex12 and also with the docking complex proteins Pex14 and Pex17. Similarly, Pex3-3HA interacted with these proteins in *pex1Δ* cells, presumably at the pER. These results confirm our previous findings showing that Pex3 is a component of both RING-domains and docking complexes in *P. pastoris* (Hazra et al., 2002). Most interestingly, in *pex19Δ* cells, Pex3-3HA did not interact with any RING-domain or docking complex proteins, suggesting a requirement of Pex19 for restoring the interaction between not only between Pex3 and the RING-domain proteins, but also the docking complex proteins (Fig. 7, A and B).

PMPs are trafficked in distinct peroxisomal vesicles

Our earlier study, using an immunoisolation procedure to capture Pex11-2HA on antibody-conjugated Sepharose beads, described the isolated and characterized ppVs carrying Pex11 and Pex3 (Agrawal et al., 2011). The vesicles isolated from *pex3Δ* cells were devoid of many PMPs otherwise found in the vesicles isolated from WT cells (Agrawal et al., 2011). However, later in *Saccharomyces cerevisiae*, two distinct ppVs were described, comprising the RING-domain and docking complex proteins, respectively, in distinct vesicles (ppV-R and ppV-D). A clear separation of the RING, docking, peroxisomal, and ER proteins was demonstrated using buoyant density sucrose gradients. It was proposed that these ppVs subsequently fuse to form import-competent peroxisomes (van der Zand et al., 2012) in a reaction requiring Pex1 and Pex6 proteins.

Previously, in the vesicles and/or peroxisomes isolated from WT *P. pastoris* cells, we detected both RING-domain and docking complex proteins copackaged together. This could be caused by a fusion event occurring before the isolation that

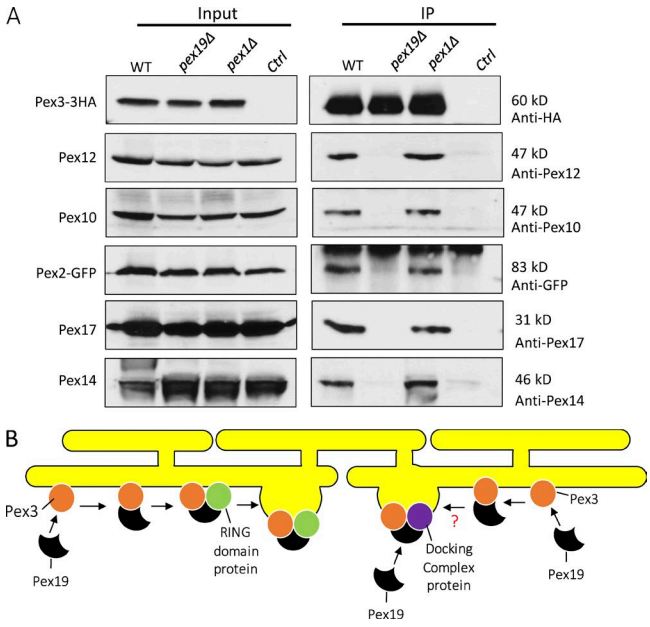

Figure 7. **Pex19 is required for the interaction between Pex3 and RING-domain, as well as docking complex, proteins.** (A) Co-IP was performed by immunoprecipitating Pex3-3HA using rat monoclonal antibodies conjugated with Sepharose beads as described in Materials and methods. The cells were harvested after 6 h in methanol medium. Coimmunoprecipitated proteins were detected by immunoblotting. Co-IP was repeated three times with similar results. (B) The updated model from Fig. 5 B depicts Pex19-dependent association of Pex3 with the docking complex proteins at the pER. This is supported by the co-IP observations in Fig. 6 A and the localization of Pex17 to the pER in *pex1Δ* cells (Fig. 5 B). The interaction of Pex3 with the docking complex proteins in *pex1Δ* cells in A suggests that Pex3 also sorts with the docking complex proteins because Pex3 is required to sort Pex10 and Pex12 into the docking complex ppVs (Fig. 8 B).

presumably reconstituted the RING-domain and docking complex proteins. Our results so far also suggested a distinct sorting mechanism for these proteins; nonetheless, heterogeneous carriers remained to be identified. Thus we sought to test whether a similar sorting and budding mechanism exists in *P. pastoris*. However, in our experiments, the buoyant density sucrose gradients did not produce a clear separation of these organellar fractions, and the ER markers and the vesicular fractions with RING-domain and docking complex proteins overlapped in *pex1Δ* and *pex6Δ* cells.

As an alternative, we immunoisolated the ppVs using either Pex2-3HA or Pex17-3HA as anchors for isolating the vesicles in strains with different genetic backgrounds (*pex19Δ*, *pex3Δ*, *pex1Δ*, *pex6Δ*, and WT). The postnuclear supernatant (PNS) after 20,000 *g* centrifugation (20S) was used for isolating the vesicles. Notably, the level of Pex2-3HA was lower compared with that of Pex17-3HA in the 20S after the cell fractionation procedure, in comparison with TCA precipitates of unbroken cells, which showed more stable Pex2-3HA. The 20S fractions were incubated with anti–rat HA monoclonal antibody conjugated to Sepharose beads and subsequently processed and analyzed as described in Materials and methods.

As expected, both Pex2-3HA and Pex17-3HA were detected in the immunoprecipitates from their respective strains, although the Pex17-3HA signal was stronger than that of Pex2-3HA (Fig. 8). Pex2-GFP was detected only in the vesicles isolated with Pex17-3HA from the WT cells, likely as a result of heterotypic fusion, but was absent in *pex1Δ* and *pex6Δ* cells (Fig. 8 A). Similarly, Pex17-GFP was detected only in the vesicles isolated with Pex2-3HA from the WT cells, but not from *pex1Δ* or *pex6Δ* cells (Fig. 8 A). In addition, the endogenous Pex17 (untagged) was present exclusively in the vesicles (membranes) isolated using Pex17-3HA, but not with those using Pex2-3HA, from *pex1Δ* and *pex6Δ* cells, showing clean separation of the ppV fractions (Fig. 8 B). Importantly, these results suggested an exclusive packaging of these PMPs, thus defining the right candidates for vesicle isolation. We also analyzed whether vesicle fusion was restored upon Pex1 reintroduction in *pex1Δ* cells. For this, we expressed Pex1 from the inducible AOX promoter in *pex1Δ* cells, also expressing Pex17-3HA and Pex2-GFP from the pGAP promoter. This strain grew on methanol and formed mature peroxisome clusters like WT cells (Fig. S4). When Pex17-3HA–containing vesicles were immunoisolated from the 20S fraction of these cells, Pex2-GFP was coisolated, but only from cells that were grown in methanol, where Pex1 was expressed (Fig. 8 A, left). These results suggest a fusion of two vesicle types upon Pex1 reintroduction, thus bringing Pex17 and Pex2 together. This was the first indication of heterogeneity in the vesicle population carrying PMPs. However, the vesicles isolated with Pex2-3HA from the WT cells showed a weak signal for Pex17, probably because of ppV fusion to form peroxisomes.

Furthermore, in our qualitative analysis, we found that the docking complex proteins, Pex13 and Pex14, were predominantly in the vesicles isolated with Pex17-3HA in *pex1Δ* and *pex6Δ* cells (Fig. 8 B). The vesicles isolated with Pex17-3HA from the WT cells had less Pex13 and Pex14, probably because of their localization in peroxisomes, which were excluded from the analysis (discarded as a part of the 20P fraction). In contrast, all the docking complex proteins, Pex13, Pex14, and Pex17, were largely absent in the vesicles isolated with Pex2-HA in *pex1Δ* and *pex6Δ* cells (Fig. 8 B).

Interestingly, Pex3 was detected in vesicles isolated with both Pex2-3HA and Pex17-3HA in WT, *pex1Δ*, and *pex6Δ* cells, suggesting that Pex3 is packaged with both RING-domain and docking complex proteins. A similar observation was reported previously in *S. cerevisiae* using buoyant density gradients (van der Zand et al., 2012). Pex19 was also present with both fractions. This was expected, as Pex19 was required for the budding of both RING-domain and docking complex proteins.

The docking complex proteins, Pex13, Pex14, and Pex17, were present in the vesicles isolated containing Pex17-HA from the *pex3Δ* cells, in agreement with the budding assay (Fig. 1 C), in which Pex3 was dispensable for the budding of these proteins. The weak signal obtained for Pex2-HA in *pex3Δ* cells was probably from membrane fragmentation of the ER, but importantly, this fraction did not contain any of the other PMPs analyzed, consistent with our idea that Pex3 is necessary for the sorting of Pex2 to the pER and for its subsequent budding into ppVs.

Pex10 and Pex12 are copackaged with the docking complex proteins

The most surprising result was the localization of Pex10 and Pex12 in the immunoisolated vesicles containing Pex17-HA (Fig. 8 B, left), because these RING-domain proteins were expected to sort with Pex2 (van der Zand et al., 2012).

In our experiments, however, Pex10 and Pex12 were exclusively detected in the vesicles isolated with Pex17-3HA in *pex1Δ* and *pex6Δ* cells (Fig. 8 B). A very weak signal for Pex12 was detected in the vesicles isolated with Pex2-3HA in the WT cells,

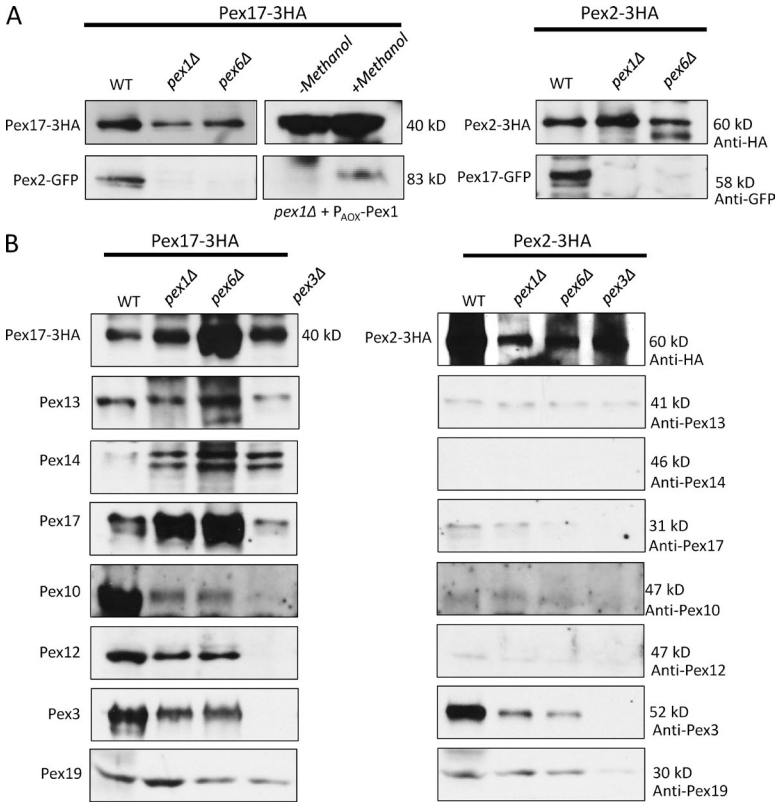

Figure 8. **Immunoisolation and protein composition of preperoxisomal vesicles.** Immunoisolation of preperoxisomal vesicles was performed as described in Materials and methods. Pex2-3HA and Pex17-3HA were used as anchors for isolation of vesicles from 20S. After antibodies coupled to Sepharose beads were used to capture the ppVs, beads were washed three times, and associated membranes were eluted in SDS sample buffer. The immunoisolate was analyzed with specified antibodies. The experiment was performed with cells harvested after 6 h in methanol medium. (A) Immunoisolation was performed with 20S fractions from WT, *pex1Δ*, and *pex6Δ* cells expressing either Pex17-3HA and Pex2-GFP or Pex2-3HA and Pex17-GFP expressed from the constitutive GAP promoter. In *pex3Δ* cells, Pex2-GFP was not detectable in the 20S fraction, probably because it is retained in the ER (Fig. 1 C) and thus was not included in the experiment. *pex1Δ* cells expressing P_{AOX}-Pex1 were switched from YPD to methanol medium (+Methanol) for 6 h or were continued in YPD (–Methanol) before immunoisolation of vesicles. (B) Immunoisolation was performed with 20S fractions from WT, *pex1Δ*, and *pex6Δ* cells expressing either Pex17-3HA or Pex2-3HA. The expression of Pex2-3HA was considerably lower than that of Pex17-3HA in *pex1Δ*, *pex6Δ*, and *pex3Δ* cells, and the blot (right) was exposed for a longer duration (~10×). The experiment was repeated more than three times with similar results.

perhaps as a result of heterotypic fusion. Importantly, Pex10 and Pex12 were not found in the Pex2-HA vesicles in *pex1Δ* and *pex6Δ* cells (Fig. 8 B, right). The exclusive association of the RING-domain proteins with the docking complex proteins is a prominent difference in the sorting of PMPs in *P. pastoris.*

Pex3 sorts Pex10 and Pex12 with the docking complex proteins

More interestingly, Pex12 was absent in the vesicles isolated from the *pex3Δ* cells using Pex17-3HA, yet the docking complex proteins, Pex14 and Pex17, were present in these vesicles. This finding is in line with our budding assay results and implies that although Pex12 was packaged with the docking complex proteins, its budding still requires Pex3, like the other RING protein, Pex2.

To address why Pex12 requires Pex3 for budding, we hypothesized that the intra-ER sorting of Pex12 to the pER might require Pex3 (as shown for Pex2; Fig. 2 A). We tagged Pex12 with GFP and localized it in *pex3Δ*, *pex19Δ*, *pex1Δ*, and *pex6Δ* cells. Interestingly, Pex12 (like Pex2) localized near the cortical ER along with Sec61-mCherry in *pex3Δ* and *pex19Δ* cells, without any punctate localization, whereas in *pex1Δ* and *pex6Δ* cells, it relocated to the punctate structure (Fig. 9), thus resembling the sorting pattern seen with Pex2 (Fig. 2 A). This clearly indicates that Pex3 and Pex19 are required for intra-ER sorting of Pex12, explaining the necessity of Pex3 for Pex12 budding into ppVs. The detection of some Pex3 in vesicles containing Pex17-3HA from *pex1Δ* and *pex6Δ* cells (Fig. 8 B) suggests that this fraction of Pex3 functions in the sorting of Pex12 from the pER to the docking complex vesicle.

Because Pex3 is essential for the sorting of Pex10 and Pex12 with the docking subcomplex, we hypothesized that in *pex3Δ* cells the interaction between these RING-domain proteins with the docking subcomplex should be disrupted. In a co-IP experiment, we immunoprecipitated Pex17-3HA in WT, *pex3Δ*, *pex19Δ*, and *pex1Δ* cells. As expected in the WT cells, Pex17-3HA showed a strong interaction with all PMPs tested (Fig. 10 A). Similarly, in *pex1Δ* cells, Pex10 and Pex12 interacted strongly with Pex17-3HA, likely at the pER. However, in *pex3Δ* cells, this interaction was completely disrupted, further confirming the role of Pex3 in the sorting of Pex10 and Pex12 with the docking complex proteins at the pER (Fig. 10 A). Interestingly, the interaction between Pex17-3HA and Pex2-GFP was not detected in any background other than the WT cells, further confirming an independent packaging of these PMPs.

It is puzzling that although the three RING-domain proteins (Pex2, Pex10, and Pex12) form a complex that is dependent on Pex3 in *P. pastoris* (Hazra et al., 2002) they are sorted at the pER into two distinct vesicles. We do not yet understand why this is so, but presumably such a mechanism would ensure that the importomer complex would not prematurely assemble at the ER. In addition, the requirement of both Pex3 and Pex19 for the intra-ER sorting and budding of all these RING proteins explains why Pex3 and Pex19 are associated with both types of vesicles in *P. pastoris*.

Discussion

The emergence of ppVs from the ER and their role in peroxisome biogenesis in eukaryotic cells is an attractive concept that explains how peroxisomes arise during the complementation of *pex* mutants that have no detectable preexisting peroxisomes (Agrawal and Subramani, 2015). Recent studies in yeast, invertebrates, and mammalian cells have discovered that many PMPs are trafficked via the ER to the peroxisome (Kim et al., 2006; Lam et al., 2010; Agrawal et al., 2011; Yonekawa et al., 2011; Kalel et al., 2015). However, the mechanisms or molecular requirements for

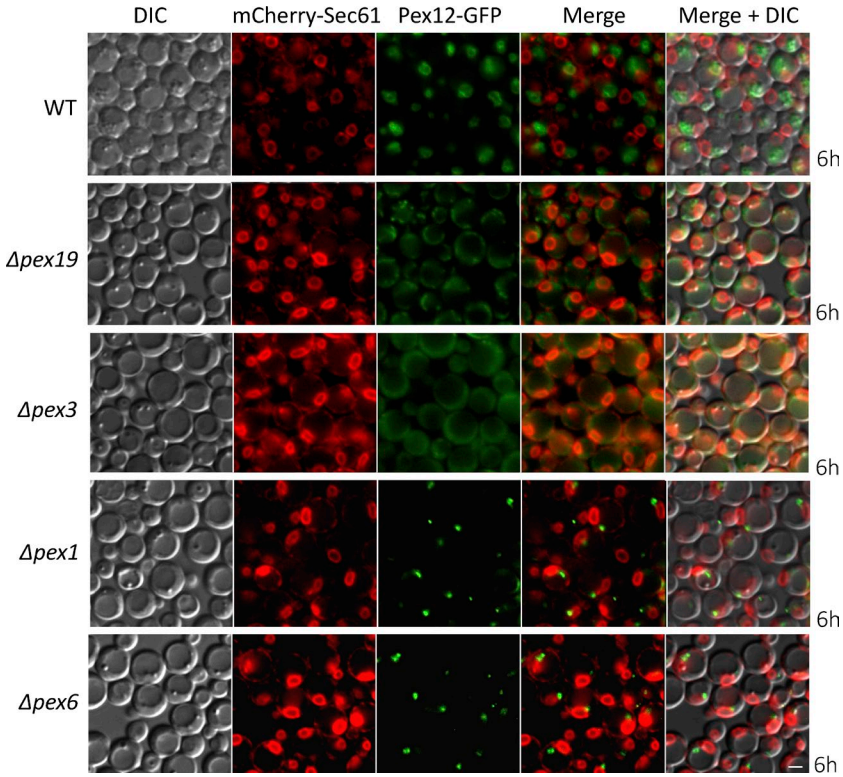

Figure 9. **Localization of Pex12-GFP in WT and mutant cells.** Pex12-GFP and mCherry-Sec61 localization in WT, *pex19Δ*, *pex3Δ*, *pex1Δ*, and *pex6Δ* cells. Bar, 2 µm. Each localization experiment was repeated three times with similar results.

such trafficking are poorly understood. Although ppV budding has been demonstrated in vitro, the preceding events of intra-ER sorting to distinct domains of the ER, and subsequent packing of PMPs into ppVs of distinct protein composition, remain unexplored mechanistically. This work defines the essential molecular apparatus functioning to allow peroxisome biogenesis at the ER. Our results highlight an extraordinary sorting process that prevents premature assembly of PMPs at the ER.

Role of Pex19 in ppV budding and bridging Pex3 interactions with docking and RING-domain subcomplex proteins

Pex19 functions as a PMP receptor that is present in all eukaryotic cells and is indispensable for peroxisome biogenesis. During the growth and division cycle in mammalian cells, Pex19 and Pex3 work together to incorporate PMPs into the peroxisomal membrane (Fang et al., 2004). This is a role for Pex19 in the cytosol. Additionally, previous studies in yeast have highlighted another role of Pex19 in de novo peroxisome biogenesis at the ER membrane. Pex19, in addition to ATP and cytosolic factors, was essential for the budding of ppVs from the ER (Fig. 1 C; Lam et al., 2010; Agrawal et al., 2011). Recently, two distinct vesicle types were identified, carrying the RING-domain and docking subcomplex proteins exclusively (van der Zand et al., 2012). It was thus imperative to test in vitro whether Pex19 is essential for the budding of both types of vesicles. Indeed, in our in vitro ER budding assays, we determined that Pex19 is required for the budding of both types of vesicles, because in *pex19Δ* cells none of the PMPs tested buds from the ER (Fig. 1 C). This result highlights the importance of Pex19 in ppV budding at the ER membrane, during de novo peroxisome biogenesis.

We also obtained evidence of an early role for Pex19 at the ER in serving as a bridge for interactions between Pex3 and both docking and RING PMPs. Pex3 was not able to interact with either the docking complex or the RING-domain proteins in *pex19Δ* cells (Fig. 7 A, right). However, in *pex1Δ* cells, this interaction remained strong. This result supports our earlier study in which we discovered Pex3 to be a part of both RING-domain and docking subcomplexes (Hazra et al., 2002).

Novel roles of Pex3 in intra-ER sorting and budding of RING-domain subcomplex proteins

Pex3, like Pex19, is indispensable for peroxisome biogenesis in all eukaryotic cells (Agrawal and Subramani, 2013). Pex3 is a multifunctional protein that functions at various steps of the growth and division pathway, including incorporation of PMPs into the peroxisomal membrane (Fang et al., 2004), stabilizing the importomer (Hazra et al., 2002), peroxisome division and segregation during cell division (Knoblach and Rachubinski, 2015), and pexophagy (Farré et al., 2008; Motley et al., 2012; Burnett et al., 2015). Pex3 is one of the first PMPs that was shown to traffic through the ER in both mammalian and yeast cells (Hoepfner et al., 2005; Tam et al., 2005; Kim et al., 2006). Because Pex3 and Pex19 work together in the growth and division pathway of peroxisome biogenesis, and *pex3Δ* cells lack functional peroxisomes, it was expected that Pex3 would play an essential role during de novo biogenesis, likely by recruiting Pex19 to the ER membrane, in its proposed role as a docking factor (Fang et al., 2004). Surprisingly, however, Pex3 was found to be dispensable for the budding of Pex11 from the ER (Fig. 1 C; Agrawal et al., 2011), and consequently, the precise role of Pex3 in the de novo peroxisome biogenesis pathway remained elusive. We show for the first time a novel role of Pex3 in intra-ER sorting and budding of RING-domain PMPs (Pex2, Pex10, and Pex12) from the ER.

Both Pex3 and Pex19 are shown here to have novel roles in the intra-ER sorting of RING-domain proteins to the pER domains. Visualization of fluorescence-tagged RING and docking

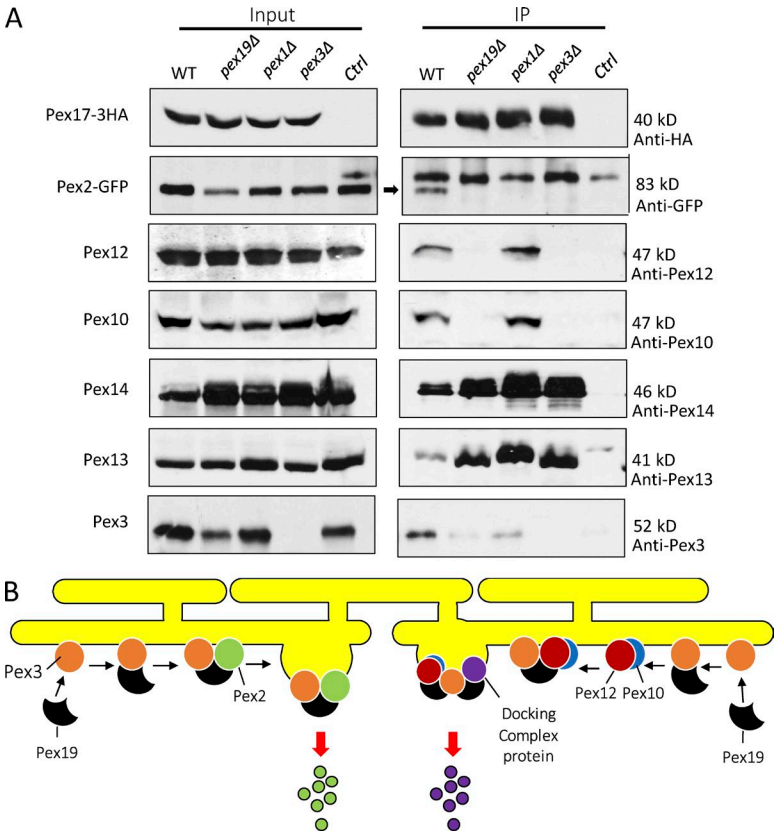

Figure 10. **Pex3 and Pex19 are required for the sorting of Pex12 into vesicles containing the docking subcomplex proteins.** (A) Interaction of Pex17-3HA with Pex3, RING-domain, and docking complex proteins in WT, *pex19Δ*, *pex3Δ*, and *pex1Δ* cells. The co-IP experiment was repeated twice with similar results. Ctrl, control. (B) Model for the role of Pex19 and Pex3 in the sorting and budding of RING-domain and docking complex proteins from the ER. Both Pex3 and Pex19 must interact with RING-domain proteins at the cortical ER to form stable ternary complexes (Figs. 6 A and 7 A), which are then sorted to the pER domains from which the distinct ppVs bud (Fig. 1 C). In the absence of either Pex3 or Pex19, the RING-domain proteins are dispersed over the cortical ER and fail to localize to the punctate pER (Figs. 2 A and 9). Because Pex3 is a membrane protein and Pex19 is a cytosolic protein that docks with Pex3, and because Pex3 has its own intra-ER sorting signal (Fakieh et al., 2013), Pex3 must sort the RING proteins to the pER. In contrast to the RING-domain proteins, neither Pex3 nor Pex19 is required for the intra-ER sorting of a docking protein, such as Pex17, to the pER (Fig. 2 B). Furthermore, although Pex3 is not necessary for the budding of ppV-D vesicles (Fig. 1 C), it is found associated with the vesicles immunoisolated with Pex17-HA (Fig. 8 B) because these vesicles contain RING-domain proteins, Pex10 and Pex12 (Fig. 8 B), whose intra-ER sorting is dependent on Pex3 and Pex19 (Fig. 9). New functions revealed for Pex3 by this study are (1) its role in de novo peroxisome biogenesis and (2) its role in the intra-ER sorting and subsequent budding of the RING-domain proteins from the pER, but not for either process for the docking complex proteins. For Pex19, we present new information that it docks with Pex3 at the ER membrane, where it both bridges and stabilizes the interactions with the RING-domain proteins, to allow intra-ER sorting of these proteins to the pER. Subsequently, as shown previously, Pex19 is also required for budding of both ppVs from the ER (Lam et al., 2010; Agrawal et al., 2011).

subcomplex proteins provided first insight into this mechanistic role of Pex3 and Pex19. A stark distinction in the localization of Pex2 and Pex17 in cells lacking Pex3, Pex19, or both was highly apparent. Pex17 was localized to a distinct punctate structure associated with the ER, perhaps representing the pER, whereas Pex2 was dispersed along the cell periphery (Fig. 2). However, in *pex1Δ* and/or *pex6Δ* cells, Pex2 was sorted properly to the pER (Fig. 5). This suggested an exclusive role of Pex3 and Pex19 in the intra-ER sorting of the RING-domain proteins, whereas the docking subcomplex proteins sort independently to the ER. Pex3 itself was localized to the pER because it contains an N-terminal pER sorting signal (Fakieh et al., 2013). Presumably, the RING-domain subcomplex might piggy-back in association with Pex3 to get sorted to the pER, whereas the docking complex proteins either contain an intra-ER sorting signal or use an as-yet-unknown protein for sorting to the pER.

The requirement of both Pex3 and Pex19 for sorting Pex2 to the pER is explained by the co-IP analysis showing that in *pex19Δ* cells, Pex3 does not interact with the RING-domain proteins at the ER (Fig. 7 A, right), suggesting that a stable ternary complex, comprised of Pex3 and the RING PMPs bridged by Pex19, is necessary for the intra-ER sorting of RING-domain PMPs to the pER domains.

In mammalian cells, Pex19 functions as a chaperone, binding and stabilizing newly synthesized PMPs in the cytoplasm through their hydrophobic domains and then inserting them into the peroxisomal membrane (Shibata et al., 2004; Kashiwayama et al., 2005). Pex3 functions as a docking protein for Pex19 on the peroxisomal membrane with an exclusive N-terminal Pex3-binding site (Fransen et al., 2005; Sato et al., 2010; Schueller et al., 2010). Pex3 functions in a similar manner at the ER, where it serves to dock Pex19, particularly for the RING-domain subcomplex proteins. We found that Pex3 is exclusively required for docking and interaction of Pex19 with the RING-domain proteins at the ER, but not for the docking complex proteins (Fig. 6 A, right). This is further supported by the budding assay results, where both Pex3 and Pex19 were necessary for the budding of Pex2 (Fig. 1 C). Taken together with previous co-IP results, we suggest that Pex3, Pex19, and the RING-domain proteins form a ternary complex at the ER (Fig. 5 C). Presumably, Pex19 initiates the sorting process by docking on Pex3 at the ER, followed by their binding to the RING-domain proteins, thus stabilizing and escorting the RING-domain proteins to the pER. Such distinct sorting requirements for the RING-domain and docking complex PMPs should ensure proper segregation of PMPs before packaging and budding.

Another new role for Pex3 emerged in the budding of the RING-domain proteins at the ER (Figs. 1 C and 8 B). Based on results published for *S. cerevisiae*, Pex2-3HA and Pex17-3HA were expected to be localized in distinct ppVs (van der Zand et al., 2012). However, although two distinct ppVs were indeed found to segregate these proteins, they exhibited a differential requirement of Pex3 for their formation (Fig. 8 B).

In *pex3Δ* cells, Pex2-3HA failed to bud from the ER, whereas the budding of Pex17-3HA and Pex11-3HA was unimpaired (Fig. 1 C), thus suggesting a new role for Pex3 in the budding of the RING-domain proteins. This suggestion was confirmed by multiple lines of experimentation showing that the intra-ER sorting, the pER domains, and the budding requirements for the docking complex and RING-domain proteins are distinct. First, Pex2 and Pex17 exhibited distinct intra-ER

sorting requirements in that Pex17 sorted to the pER independent of either Pex3 or Pex19, whereas Pex2 sorting to the punctate pER required both Pex3 and Pex19 (Figs. 2 and 5). Mechanistically, this was confirmed by the fact that co-IP of Pex19 (Fig. 5 A) and Pex3 (Fig. 7 A) with the RING-domain proteins required both Pex3 and Pex19. In contrast, although the interaction of Pex3 with the docking complex PMPs required Pex19, the interaction of these PMPs with Pex19 was independent of Pex3 (Fig. 7 A).

Second, Pex2 and Pex17 localized to distinct, but adjacent, domains of the pER. Proof of this distinct localization came from fluorescence microscopic localization (Figs. 5 and S2 B) and co-IP experiments (Fig. 10 A) in *pex1Δ*, in which the RING-domain and docking complex proteins should be at the ER at early times after peroxisome induction, because the absence of the AAA ATPases should prevent ppV fusion. In such experiments, Pex2 and Pex17 were in distinct, but nonoverlapping, punctate pER structures. Additionally, immunoprecipitates of Pex17 did not contain Pex2 and vice versa (Fig. 8 A).

Finally, the presence of ppVs with distinct protein composition, different from what has been reported for *S. cerevisiae* (van der Zand et al., 2012), was confirmed by budding assays (Fig. 1), characterization of immunoisolated vesicles (Fig. 8 B), and co-IP experiments (Fig. 10 A) performed with WT and mutant yeast strains. As stated earlier, although Pex19 is important for the budding of ppVs containing Pex17, Pex3 is not. In contrast, vesicles containing Pex2 require both Pex3 and Pex19.

Different RING-domain subcomplex proteins are sorted into distinct ppVs

In *S. cerevisiae,* a clear segregation was described for RING-domain and docking subcomplex proteins, exclusively packaged into distinct vesicular carriers, presumably while trafficking these proteins out of the ER (van der Zand et al., 2012). However, our results in *P. pastoris* suggest a significantly different sorting outcome for the RING-domain subcomplex PMPs. Immunoisolation of ppVs with Pex2-3HA and Pex17-3HA showed that both Pex10 and Pex12, respectively, copackaged with the docking subcomplex proteins, and segregated away from Pex2, but the docking complex PMPs were present almost exclusively in the vesicles isolated with Pex17-3HA (Fig. 8 B). Interestingly, Pex3 was present in vesicles isolated with both Pex2-3HA and Pex17-3HA. This explained the interaction of Pex3 with both RING-domain and docking subcomplex PMPs at the pER (Fig. 7). Probably, the portion of Pex3 that sorts with the docking complex proteins brings along Pex10 and Pex12.

Even though Pex10 and Pex12 were uncharacteristically sorted with the docking subcomplex, multiple lines of evidence suggest that Pex3 and Pex19 are required, as they are for Pex2, for their intra-ER sorting and budding. First, in the vesicle isolation assay, Pex10 and Pex12 were absent in the ppVs isolated with Pex17-3HA in *pex3Δ* cells, clearly demonstrating the requirement of Pex3 for sorting, packaging, and budding of the RING-domain proteins (Fig. 8 B). Second, when Pex17-3HA was immunoprecipitated, Pex10 and Pex12 did not interact in *pex3Δ* cells, whereas Pex17-3HA retained interaction with other docking complex proteins, suggesting the requirement of Pex3 for sorting of Pex10 and Pex12 along the docking subcomplex proteins (Figs. 9 and 10). Finally, Pex12-GFP showed localization identical to that of fluorescence-tagged Pex2 in *pex3Δ* and *pex19Δ* cells, where it was dispersed toward the cell periphery with Sec61-mCherry and failed to localize to the pER (Fig. 9). Together, these observations suggest a model in which, despite their atypical copackaging, Pex10 and Pex12 resemble Pex2 in requiring Pex3 and Pex19 for intra-ER sorting, copackaging, and budding (Fig. 10 B). In contrast, the sorting of the docking complex to the pER is independent of Pex3 and Pex19, but the budding of ppVs containing these proteins requires Pex19. It will be interesting to compare the detailed protein and lipid compositions of the purified ppV populations. Indeed, this is the direction in which our future work is headed.

Materials and methods

Yeast strains and growth conditions

Yeast cells were grown at 30°C in YPD medium (1% yeast extract, 2% peptone, and 2% glucose) for the preparation of S1 fractions to OD 1.2–2.0 and transferred to methanol medium (0.67% yeast nitrogen base without amino acids, 0.02 g L-histidine/l, 0.02 g L-arginine/l, 0.1% yeast extract, and 0.5% (vol/vol) methanol for 6 h.

Fluorescence microscopy

Cells were grown on YPD and switched to methanol medium during exponential phase. Images were captured using a Plan Apochromat 100× 1.40-NA oil immersion objective on a motorized fluorescence microscope (Axioskop 2 MOT plus; Carl Zeiss) coupled to a monochrome digital camera (AxioCam MRm; Carl Zeiss) and processed using AxioVision software (version 4.5; Carl Zeiss).

In vitro ER-budding assay

The assay was preformed as described previously (Agrawal et al., 2011). In brief, cells grown overnight in YPD were harvested and induced for peroxisome biogenesis in methanol medium for 6 h to prepare the S1 fraction and 3 h to prepare PYCs. Cells were harvested (3,000 rpm for 5 min) at RT, resuspended in low-glucose medium (YP medium with 0.1% glucose), and incubated for 30 min at 25°C (50 ml per 75 OD_{600} units). Cells were pelleted, and spheroplasting was performed as described previously (Groesch et al., 1992). These regenerated spheroplasts were used to prepare permeabilized cells (75 OD_{600} units) and S1 (1500 OD_{600} units). All subsequent steps were performed at 4°C. To prepare the permeabilized cells, the spheroplasts were resuspended in 5 ml permeabilization buffer (0.1 M potassium acetate, 0.2 M sorbitol, 2 mM magnesium chloride, and 20 mM Hepes, pH 7.2), and centrifuged at 3,000 rpm for 5 min. The supernatant was carefully removed, and the pellet was resuspended in 50 µl CB+DTT buffer (250 mM sucrose, 4 mM DTT, 1 mM EGTA, and 20 mM Hepes, pH 7.4) with 1× protease inhibitor cocktail (PIC; P8215; Sigma-Aldrich) with NaF (50 mM), leupeptin (12.5 µg/ml), aprotinin (50 µg/ml), and PMSF (1 mM). To prepare the S1 fraction, the regenerated spheroplasts (1,500 OD_{600} units) were resuspended (with gentle vortexing) in 3.36 ml of 20 mM Hepes, pH 7.2, and centrifuged at 1,000 rpm for 10 min. Before the budding assay, the final concentration of buffer in each fraction was adjusted to 115 mM potassium acetate, 2.5 mM magnesium chloride, 0.2 M sorbitol, 1× PIC, and 35 mM Hepes, pH 7.2. The protein concentration was estimated using Bradford assay (Bradford, 1976) with BSA as standard.

Permeabilized cells were washed twice with TBPS (115 mM potassium acetate, 2.5 mM magnesium acetate, 0.25 M sorbitol, 1× PIC, and 25 mM Hepes, pH 7.2) and resuspended as ∼4.5 OD_{600} per 25-µl reaction. The budding reaction contained ∼4.5 OD_{600} per 25 µl PYCs, 1 mg S1 fraction (as measured with the Bradford assay), and ATP-regenerating system (1 mM ATP, 0.1 mM GTP, 20 mM creatine phosphate, and 0.2 mg/ml creatine phosphate kinase) in a

80-µl total reaction volume. The reaction mixture was incubated at 20°C for 90 min and then terminated by chilling on ice. To deplete samples of ATP, apyrase (A6410; Sigma-Aldrich) was added instead of the ATP-regenerating system. After the reaction, PYCs were pelleted by spinning the reaction at 13,000 rpm for 1 min. The supernatant was resuspended in SDS sample buffer, heated, and analyzed on 12% SDS PAGE. Immunoblotting was performed with appropriate antibodies.

TCA precipitation and subcellular fractionation

Cells were grown in YPD and switched to methanol medium (8 h) before the procedure. For TCA precipitation, 2 OD_{600} cells were harvested, and 145 µl of 100% TCA was added and stored overnight at −80°C. The next day, the cells were pelleted and washed twice with 80% acetone. The pellets were air-dried and resuspended in 2× SDS sample buffer and analyzed by SDS-PAGE followed by Western blotting with anti-GFP antibody (Roche; Fig. 4 A). For subcellular fractionations, methanol-induced cells (350 OD_{600} units) were pelleted and spheroplasted in Zymolase buffer (0.5 M KCl, 5 mM MOPS/KOH buffer, pH 7.2, and 10 mM Na_2SO_3) with Zymolase-100T (0.5 mg Zymolase per g of cells, 4 ml Zymolase buffer). Cells were then pelleted at 2200 *g*, 4°C, and resuspended in homogenization buffer (5 mM MES/KOH, pH 5.5, with 1 M sorbitol and 20 mM EDTA, pH 8.0) and gently lysed with a Dounce homogenizer (20 strokes). Unbroken cells and nuclear material were removed by spinning the lysate at 1000 *g* for 10 min (repeated three times) to form PNS. PNS was spun again at 20,000 *g* for 0.5 h to form 20P and 20S. The pellet was resuspended in equal volume as the 20S. Similarly, 20S was further spun in an ultracentrifuge (Optima MAX-E, MLA 130 rotor; Beckman Coulter) at 200,000 *g* for 0.5 h to obtain 200P and 200S. All the spins were performed at 4°C. TCA precipitates were prepared from all fractions, and equivalent volumes of each fraction were analyzed by SDS-PAGE and Western blotting with anti-GFP antibody (Roche). Because the expression of *pex3Δ*, *pex19Δ*, and *pex3Δ-pex19Δ* was lower compared with WT cells for both Pex2-GFP and Pex17-GFP, twice the amount of each fraction was analyzed for the mutant strains, and the blots were developed with femto-sensitivity ECL; the WT blots were developed with regular (nano-sensitivity) ECL (Fig. 4, B and C).

Affinity capture of ppVs

Approximately 400 OD_{600} units of cells were grown, harvested, and processed as described to obtain the 20S fraction that was used for isolating the vesicles. Notably, the level of Pex2-3HA was lower compared with Pex17-3HA in the 20S, likely a result of inefficient budding. The 20S fractions were incubated with anti–rat HA monoclonal antibody conjugated to Sepharose beads (80 µl slurry; EZview Red Affinity matrix; E6779; Sigma-Aldrich) for 3 h at 4°C. After the incubation, beads were spun at 500 *g*, and the supernatant was removed. The beads were then washed five times with homogenization buffer. Bound vesicles were solubilized and eluted with the addition of 150 µl of 1× nonreducing sample buffer and heating at 65°C. The eluate was analyzed by SDS-PAGE followed by Western blotting with specified antibodies.

Co-IP

Cells were grown on YPD to an OD_{600} of 1.5–2.5 and switched to methanol media. For all the co-IPs, ∼350 OD_{600} unit cells were used. Cells were resuspended in 2 ml IP-lysis buffer (20 mM Hepes-KOH, pH 7.4, 0.15 M NaCl, 1% CHAPS, 5 mM NaF, 50 µg/ml leupeptin, 50 µg/ml aprotinin, 1 mM PMSF, and yeast PIC with 20 mM EDTA, pH 8.0). Cells were lysed by vortexing with acid-washed glass beads. Lysate was then solubilized for an hour at 4°C with rotation. The lysate was centrifuged at 20,000 *g* for 20 min. For Pex19-FLAG co-IP (Fig. 6), cells were lysed in IP-lysis buffer without CHAPS, and the lysate was spun at 20,000 *g*. The supernatant was removed, and the pellet of the 20,000 *g* spin (20P) was solubilized with IP-lysis buffer with 1% CHAPS. The lysate was incubated with specified antibody affinity matrix (EZview Red Anti-HA Affinity matrix [E6779; Sigma-Aldrich] for IP of Pex17-3HA and Pex2-3HA; EZview Red Anti-FLAG M2 Affinity matrix [F2426; Sigma-Aldrich] for Pex19-FLAG). Lysates were incubated for 3 h at 4°C. The beads were then washed 5× with IP lysis buffer, and proteins were eluted with the addition of 150 µl of 1× nonreducing sample buffer and heating at 65°C. The eluate was analyzed by SDS-PAGE followed by Western blotting with specified antibodies.

Online supplemental material

Figs. S1 and S2 show fluorescence microscopy analysis (MIP images) of Pex2 and Pex17 in different mutant strains. Fig. S3 shows fluorescence microscopy localization of Pex2 and Pex17 in *pex1Δ* cells. Fig. S4 shows that P_{AOX}-Pex1 can functionally complement *pex1Δ* cells. Online supplemental material is available at http://www.jcb.org/cgi/content/full/jcb.201506141/DC1.

Acknowledgments

We thank members of the Subramani laboratory for their critical input.

This work was supported by National Institutes of Health grant RO1DK41737 to S. Subramani.

The authors declare no competing financial interests.

Submitted: 30 June 2015
Accepted: 5 January 2016

Note added in proof. While this manuscript was under revision, two articles were published in *The Journal of Cell Biology* (Knoops et al. 2015. *J. Cell Biol.* http://dx.doi.org/10.1083/jcb.201506059; Motley et al. 2015. *J. Cell Biol.* http://dx.doi.org/10.1083/jcb.201412066) that analyzed the role of Pex1/Pex6 in peroxisome biogenesis in *S. cerevisiae*. The findings suggest that Pex1 and Pex6 are involved in the import of peroxisomal matrix proteins but not in fusion of heterotypic ppVs. In addition, the authors failed to obtain evidence for unfused ppVs in *pex1*Δ and *pex6*Δ cells as observed by us and previously by others (Titorenko and Rachubinski. 2000. *J. Cell Biol.* http://dx.doi.org/10.1083/jcb.150.4.881; van der Zand et al. 2012. *Mol. Biol. Cell.* http://dx.doi.org/10.1091/mbc.E10-02-0082). These studies colocalized RING-domain and docking complex PMPs to similar structures in *pex1*Δ and *pex6*Δ cells at 16 h in peroxisome proliferation medium. In our studies performed with *P. pastoris*, we also observed a partial colocalization at early time points (6–16 h). At later times, however, we did observe Pex2 or Pex17 in distinct vesicular structures. In addition, we have used unique biochemical approaches to analyze these ppVs by immunoisolation from the 20S fraction and found Pex2 and Pex17 in distinct vesicular carriers in *pex1*Δ and *pex6*Δ cells. Nonetheless, we do find other RING-domain proteins, Pex10 and Pex12, to be associated with the docking complex vesicles, which is in accord with the new studies. In addition, another study in mammalian cells discovered that Pex3 was cotranslationally integrated into the ER and exited the ER in ppVs (Mayerhofer et al. 2015. *Traffic.* http://dx.doi.org/10.1111/tra.12350).

References

Agrawal, G., and S. Subramani. 2013. Emerging role of the endoplasmic reticulum in peroxisome biogenesis. *Front. Physiol.* 4:286. http://dx.doi.org/10.3389/fphys.2013.00286

Agrawal, G., and S. Subramani. 2015. De novo peroxisome biogenesis: Evolving concepts and conundrums. *Biochim. Biophys. Acta.* http://dx.doi.org/10.1016/j.bbamcr.2015.09.014

Agrawal, G., S. Joshi, and S. Subramani. 2011. Cell-free sorting of peroxisomal membrane proteins from the endoplasmic reticulum. *Proc. Natl. Acad. Sci. USA.* 108:9113–9118. http://dx.doi.org/10.1073/pnas.1018749108

Bradford, M.M. 1976. A rapid and sensitive method for the quantitation of microgram quantities of protein utilizing the principle of protein-dye binding. *Anal. Biochem.* 72:248–254. http://dx.doi.org/10.1016/0003-2697(76)90527-3

Burnett, S.F., J.-C. Farré, T.Y. Nazarko, and S. Subramani. 2015. Peroxisomal Pex3 activates selective autophagy of peroxisomes via interaction with the pexophagy receptor Atg30. *J. Biol. Chem.* 290:8623–8631. http://dx.doi.org/10.1074/jbc.M114.619338

Faber, K.N., J.A. Heyman, and S. Subramani. 1998. Two AAA family peroxins, PpPex1p and PpPex6p, interact with each other in an ATP-dependent manner and are associated with different subcellular membranous structures distinct from peroxisomes. *Mol. Cell. Biol.* 18:936–943. http://dx.doi.org/10.1128/MCB.18.2.936

Fakieh, M.H., P.J.M. Drake, J. Lacey, J.M. Munck, A.M. Motley, and E.H. Hettema. 2013. Intra-ER sorting of the peroxisomal membrane protein Pex3 relies on its luminal domain. *Biol. Open.* 2:829–837. http://dx.doi.org/10.1242/bio.20134788

Fang, Y., J.C. Morrell, J.M. Jones, and S.J. Gould. 2004. PEX3 functions as a PEX19 docking factor in the import of class I peroxisomal membrane proteins. *J. Cell Biol.* 164:863–875. http://dx.doi.org/10.1083/jcb.200311131

Farré, J.-C., R. Manjithaya, R.D. Mathewson, and S. Subramani. 2008. PpAtg30 tags peroxisomes for turnover by selective autophagy. *Dev. Cell.* 14:365–376. http://dx.doi.org/10.1016/j.devcel.2007.12.011

Fransen, M., I. Vastiau, C. Brees, V. Brys, G.P. Mannaerts, and P.P. Van Veldhoven. 2005. Analysis of human Pex19p's domain structure by pentapeptide scanning mutagenesis. *J. Mol. Biol.* 346:1275–1286. http://dx.doi.org/10.1016/j.jmb.2005.01.013

Fujiki, Y., K. Okumoto, S. Mukai, M. Honsho, and S. Tamura. 2014. Peroxisome biogenesis in mammalian cells. *Front. Physiol.* 5:307. http://dx.doi.org/10.3389/fphys.2014.00307

Groesch, M.E., G. Rossi, and S. Ferro-Novick. 1992. Reconstitution of endoplasmic reticulum to Golgi transport in yeast: In vitro assay to characterize secretory mutants and functional transport vesicles. *Methods Enzymol.* 219:137–152. http://dx.doi.org/10.1016/0076-6879(92)19016-Y

Hazra, P.P., I. Suriapranata, W.B. Snyder, and S. Subramani. 2002. Peroxisome remnants in pex3delta cells and the requirement of Pex3p for interactions between the peroxisomal docking and translocation subcomplexes. *Traffic.* 3:560–574. http://dx.doi.org/10.1034/j.1600-0854.2002.30806.x

Hoepfner, D., D. Schildknegt, I. Braakman, P. Philippsen, and H.F. Tabak. 2005. Contribution of the endoplasmic reticulum to peroxisome formation. *Cell.* 122:85–95. http://dx.doi.org/10.1016/j.cell.2005.04.025

Kalel, V.C., W. Schliebs, and R. Erdmann. 2015. Identification and functional characterization of *Trypanosoma brucei* peroxin 16. *Biochim. Biophys. Acta.* 1853(10, 10 Pt A):2326–2337. http://dx.doi.org/10.1016/j.bbamcr.2015.05.024

Kashiwayama, Y., K. Asahina, H. Shibata, M. Morita, A.C. Muntau, A.A. Roscher, R.J.A. Wanders, N. Shimozawa, M. Sakaguchi, H. Kato, and T. Imanaka. 2005. Role of Pex19p in the targeting of PMP70 to peroxisome. *Biochim. Biophys. Acta.* 1746:116–128. http://dx.doi.org/10.1016/j.bbamcr.2005.10.006

Kim, P.K., and E.H. Hettema. 2015. Multiple pathways for protein transport to peroxisomes. *J. Mol. Biol.* 427(6, 6 Pt A):1176–1190. http://dx.doi.org/10.1016/j.jmb.2015.02.005

Kim, P.K., R.T. Mullen, U. Schumann, and J. Lippincott-Schwartz. 2006. The origin and maintenance of mammalian peroxisomes involves a de novo PEX16-dependent pathway from the ER. *J. Cell Biol.* 173:521–532. http://dx.doi.org/10.1083/jcb.200601036

Knoblach, B., and R.A. Rachubinski. 2015. Sharing the cell's bounty—organelle inheritance in yeast. *J. Cell Sci.* 128:621–630. http://dx.doi.org/10.1242/jcs.151423

Lam, S.K., N. Yoda, and R. Schekman. 2010. A vesicle carrier that mediates peroxisome protein traffic from the endoplasmic reticulum. *Proc. Natl. Acad. Sci. USA.* 107:21523–21528. http://dx.doi.org/10.1073/pnas.1013397107

Lazarow, P.B.P. 1989. Peroxisome biogenesis. *Curr. Opin. Cell Biol.* 1:630–634. http://dx.doi.org/10.1016/0955-0674(89)90026-4

Lazarow, P.B., and Y. Fujiki. 1985. Biogenesis of peroxisomes. *Annu. Rev. Cell Biol.* 1:489–530. http://dx.doi.org/10.1146/annurev.cb.01.110185.002421

Motley, A.M., J.M. Nuttall, and E.H. Hettema. 2012. Pex3-anchored Atg36 tags peroxisomes for degradation in *Saccharomyces cerevisiae*. *EMBO J.* 31:2852–2868. http://dx.doi.org/10.1038/emboj.2012.151

Sato, Y., H. Shibata, T. Nakatsu, H. Nakano, Y. Kashiwayama, T. Imanaka, and H. Kato. 2010. Structural basis for docking of peroxisomal membrane protein carrier Pex19p onto its receptor Pex3p. *EMBO J.* 29:4083–4093. http://dx.doi.org/10.1038/emboj.2010.293

Schueller, N., S.J. Holton, K. Fodor, M. Milewski, P. Konarev, W.A. Stanley, J. Wolf, R. Erdmann, W. Schliebs, Y.H. Song, and M. Wilmanns. 2010. The peroxisomal receptor Pex19p forms a helical mPTS recognition domain. *EMBO J.* 29:2491–2500. http://dx.doi.org/10.1038/emboj.2010.115

Shibata, H., Y. Kashiwayama, T. Imanaka, and H. Kato. 2004. Domain architecture and activity of human Pex19p, a chaperone-like protein for intracellular trafficking of peroxisomal membrane proteins. *J. Biol. Chem.* 279:38486–38494. http://dx.doi.org/10.1074/jbc.M402204200

Snyder, W.B., A. Koller, A.J. Choy, and S. Subramani. 2000. The peroxin Pex19p interacts with multiple, integral membrane proteins at the peroxisomal membrane. *J. Cell Biol.* 149:1171–1178. http://dx.doi.org/10.1083/jcb.149.6.1171

Tabak, H.F., I. Braakman, and A. van der Zand. 2013. Peroxisome formation and maintenance are dependent on the endoplasmic reticulum. *Annu. Rev. Biochem.* 82:723–744. http://dx.doi.org/10.1146/annurev-biochem-081111-125123

Tam, Y.Y., A. Fagarasanu, M. Fagarasanu, and R.A. Rachubinski. 2005. Pex3p initiates the formation of a preperoxisomal compartment from a subdomain of the endoplasmic reticulum in *Saccharomyces cerevisiae*. *J. Biol. Chem.* 280:34933–34939. http://dx.doi.org/10.1074/jbc.M506208200

Titorenko, V.I., and R.A. Rachubinski. 1998. Mutants of the yeast *Yarrowia lipolytica* defective in protein exit from the endoplasmic reticulum are also defective in peroxisome biogenesis. *Mol. Cell. Biol.* 18:2789–2803. http://dx.doi.org/10.1128/MCB.18.5.2789

Titorenko, V.I., and R.A. Rachubinski. 2000. Peroxisomal membrane fusion requires two AAA family ATPases, Pex1p and Pex6p. *J. Cell Biol.* 150:881–886. http://dx.doi.org/10.1083/jcb.150.4.881

van der Zand, A., I. Braakman, and H.F. Tabak. 2010. Peroxisomal membrane proteins insert into the endoplasmic reticulum. *Mol. Biol. Cell.* 21:2057–2065. http://dx.doi.org/10.1091/mbc.E10-02-0082

van der Zand, A., J. Gent, I. Braakman, and H.F. Tabak. 2012. Biochemically distinct vesicles from the endoplasmic reticulum fuse to form peroxisomes. *Cell.* 149:397–409. http://dx.doi.org/10.1016/j.cell.2012.01.054

Yan, M., D.A. Rachubinski, S. Joshi, R.A. Rachubinski, and S. Subramani. 2008. Dysferlin domain-containing proteins, Pex30p and Pex31p, localized to two compartments, control the number and size of oleate-induced peroxisomes in *Pichia pastoris*. *Mol. Biol. Cell.* 19:885–898. http://dx.doi.org/10.1091/mbc.E07-10-1042

Yonekawa, S., A. Furuno, T. Baba, Y. Fujiki, Y. Ogasawara, A. Yamamoto, M. Tagaya, and K. Tani. 2011. Sec16B is involved in the endoplasmic reticulum export of the peroxisomal membrane biogenesis factor peroxin 16 (Pex16) in mammalian cells. *Proc. Natl. Acad. Sci. USA.* 108:12746–12751. http://dx.doi.org/10.1073/pnas.1103283108